

Orthogonal Protein Decoration of DNA Origami**

Barbara Saccà, Rebecca Meyer, Michael Erkelenz, Kathrin Kiko, Andreas Arndt, Hendrik Schroeder, Kersten S. Rabe, and Christof M. Niemeyer*

Structural DNA nanotechnology^[1,2] and the technique of DNA origami^[3] enable the rapid generation of a plethora of complex self-assembled nanostructures.^[4–6] Since DNA molecules themselves display limited chemical, optical, and electronic functionality, it is of utmost importance to devise methods to decorate DNA scaffolds with functional moieties to realize applications in sensing, catalysis, and device fabrication. Protein functionalization is particularly desirable because it allows exploitation of an almost unlimited variety of functional elements which nature has evolved over billions of years.^[7] The delicate architecture of proteins has resulted in no generally applicable method being currently available to selectively couple these components on DNA scaffolds, and thus approaches used so far are based on reversible antibody–antigen interactions,^[8,9] aptamer binding,^[10,11] nucleic acid hybridization of DNA-tagged proteins,^[12,13] or predominantly biotin–streptavidin (STV) interactions.^[14–19] We demonstrate here that DNA nanostructures can be site-specifically decorated with several different proteins by using coupling systems orthogonal to the biotin–STV system. In particular, benzylguanine (BG) and chlorohexane (CH) groups incorporated in DNA origami have been used as suicide ligands for the site-specific coupling of fusion proteins containing the self-labeling protein tags O⁶-alkylguanine-DNA-alkyltransferase (hAGT), which is often referred to as “Snap-tag”,^[20] or haloalkane dehalogenase, which is also known as “Halo-Tag”.^[21] By using various model proteins we demonstrate the general applicability of this approach for the generation of DNA superstructures that are selectively decorated with multiple different proteins.

To realize orthogonal protein immobilization on DNA origami using self-ligating protein tags, we chose the Snap-tag, developed by Johnsson and co-workers,^[20] and the commercially available HaloTag^[21] system. The respective small-molecule suicide tags (O⁶-benzylguanine (BG) and 5-chlorohexane (CH)) for both self-labeling protein tags are readily available as amino-reactive *N*-hydroxysuccinimide (NHS) derivatives (BG-NHS and CH-NHS; Figure 1a). Complete derivatization of alkylamino-modified oligonucleotides was achieved by coupling with 30 molar equivalents of BG-NHS or CH-NHS, as indicated by electrophoretic analysis (Figure 1b). To gain access to fusion proteins bearing the complementary Snap- and Halo-protein tags, we constructed expression plasmids by genetic fusion of the genes encoding the protein of interest (POI) and Snap-tag or HaloTag (see the Supporting Information). As model POIs we chose the fluorescent proteins enhanced yellow fluorescent protein (EYFP)^[22] and mKate,^[23] the enzymes cytochrome C peroxidase (CCP)^[24] and esterase 2 from *Alicyclobacillus acidocaldarius thermos* (EST2),^[25] to which the self-labeling tags were fused at the C terminus (POI-Snap or POI-Halo, respectively). In addition, the bispecific Halo-Snap fusion protein “covalin”,^[26] a chimera which specifically reacts with both BG and CH, as well as monovalent STV (mSTV),^[27] were used in this study. The fusion proteins were overexpressed and purified by conventional procedures (see the Supporting Information). The coupling of BG- and CH-modified oligonucleotides to the protein was analyzed by using covalin as the initial model to simplify the electrophoretic characterization. It is shown in Figure 1c that both BG- and CH-modified single-stranded DNA (ssDNA) oligonucleotides couple effectively to generate the corresponding DNA–covalin conjugates in nearly quantitative yields. DNA coupling of the aforementioned POI fusions, namely mKate-Snap, EST2-SNAP, mKate-Halo, CCP-Halo, and EYFP-Halo occurred in a highly specific manner (Figure 1d), and neither Snap or Halo nor mSTV revealed cross-reactivity for the orthogonal-tagged DNA oligomers.

We then used SARSE software to aid in the design of face-shaped DNA origami to demonstrate the selective immobilization of protein on DNA nanostructures.^[28] Correct folding of M13mp18 ssDNA through the use of 236 staple strands was analyzed by atomic force microscopy (AFM); details of the sequence design as well as experimental procedures are reported in the Supporting Information). Figure 2a illustrates that the face-shaped DNA origami was obtained in high purity, and high-resolution AFM clearly revealed the proposed ears, neck, and seam features of this structure. As an initial test for protein decoration, we selected 23 staple strands, which were biotinylated to create eyes (2 × 6

[*] Dr. B. Saccà,^[†] Dipl.-Chem. R. Meyer,^[†] Dipl.-Biotechnol. M. Erkelenz, M. Sc. K. Kiko, A. Arndt, Dr. H. Schroeder, Dr. K. S. Rabe, Prof. C. M. Niemeyer
Technische Universität Dortmund, Fakultät Chemie
Biologisch-Chemische Mikrostrukturtechnik
Otto-Hahn Strasse 6, 44227 Dortmund (Germany)
Fax: (+49) 231-755-7082
E-mail: christof.niemeyer@tu-dortmund.de

[†] These authors contributed equally to this work.

[**] This work was supported by the Deutsche Forschungsgemeinschaft (SA 1952/1-1, NI 399/10-1) and the Max-Planck Society (fellowship to C.M.N.). We are most grateful to Prof. Kai Johnsson for the generous donation of the covalin expression plasmid and helpful discussions. We also thank Prof. Mathias Sprinzl for kind donation of a plasmid encoding for EST2, and Dr. Michael Adler for help with IPCR analyses. Stephanie Reisewitz and Julian Engel are acknowledged for experimental support in cloning.



Supporting information for this article is available on the WWW under <http://dx.doi.org/10.1002/anie.201005931>.

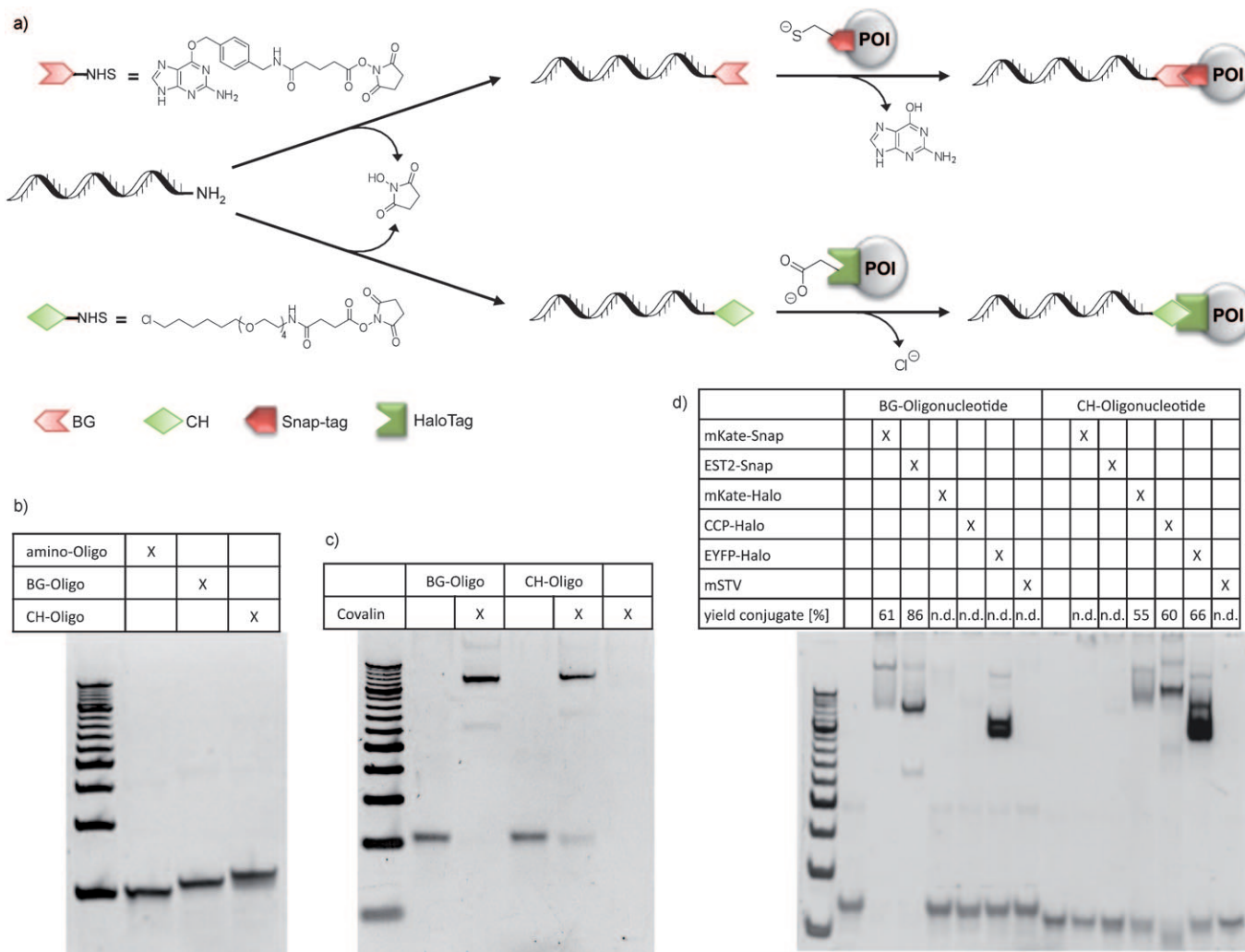


Figure 1. a) Schematic representation of chemical coupling of amino-modified DNA oligonucleotides with benzylguanine (BG) or chlorohexane (CH) groups as orthogonal tags for modification of proteins of interest (POI) genetically fused with Snap-tag or HaloTag, respectively, at the C termini. b) Complete reaction of the amino-modified DNA oligomers with BG and CH is demonstrated by electrophoresis on a 20% denaturing polyacrylamide gel. Electrophoresis on 10% polyacrylamide gels shows the selective coupling of BG- or CH-modified oligomers with c) chimeric Snap-tag/HaloTag fusion covalin or d) POI-Snap-tag and POI-HaloTag fusions. n.d. = not detectable. For additional protein binding studies see Figure S2 in the Supporting Information.

strands), a nose (4 strands), and a mouth (7 strands) on the facelike origami (Figure 2b and see Figure S3 in the Supporting Information). Subsequent to assembly, the biotinylated DNA origami was adsorbed onto mica and mSTV was allowed to bind. AFM analysis revealed the expected smiley face structures in addition to unmodified structures in approximately equal amounts (Figure 2c and see Table S9 in the Supporting Information). The presence of both fully modified and unmodified structures results from an equally favored face-up and face-down orientation (Figure 2e, upper and lower panel, respectively) during adsorption of oligobiotinylated structures on mica substrates. However, since polyanionic DNA structures have a higher affinity for mica than STV (isoelectric point, $pI \approx 6$), modification of the structure with mSTV in homogenous solution, followed by their adsorption onto mica, led almost exclusively to face-up-oriented nanostructures (Figure 2d).

To investigate whether incorporated BG-, CH-, and biotin-derivatized staple strands can be used for orthogonal

protein decoration of the origami we assembled a face-shaped origami of similar design as depicted in Figure 2b, in which the eyes, nose, and mouth features were encoded by two times three CH-, four biotin-, and four BG-bearing oligomers, respectively (Figure 3 and see Figure S4 in the Supporting Information). Subsequent to assembly, the origami was incubated with CCP-Halo (Figure 3a), mSTV (Figure 3b), mKate-Snap (Figure 3c), or covalin (Figure 3d). AFM imaging of the resulting structures clearly indicated that protein binding occurred exclusively at the positions containing the complementary small-molecule tags. We also demonstrate that orthogonal protein binding can be achieved by consecutive binding events. The BG-, CH-, and biotin-bearing origami (Figure 3e) was initially labeled with mKate-Snap, thus giving rise to the mouth feature (Figure 3f). This origami was then allowed to bind CCP-Halo, which led to appearance of the eye features (Figure 3g). Finally, treatment with mSTV led to formation of the fully decorated smiley face structure (Figure 3h). Stepwise addition of different proteins to the

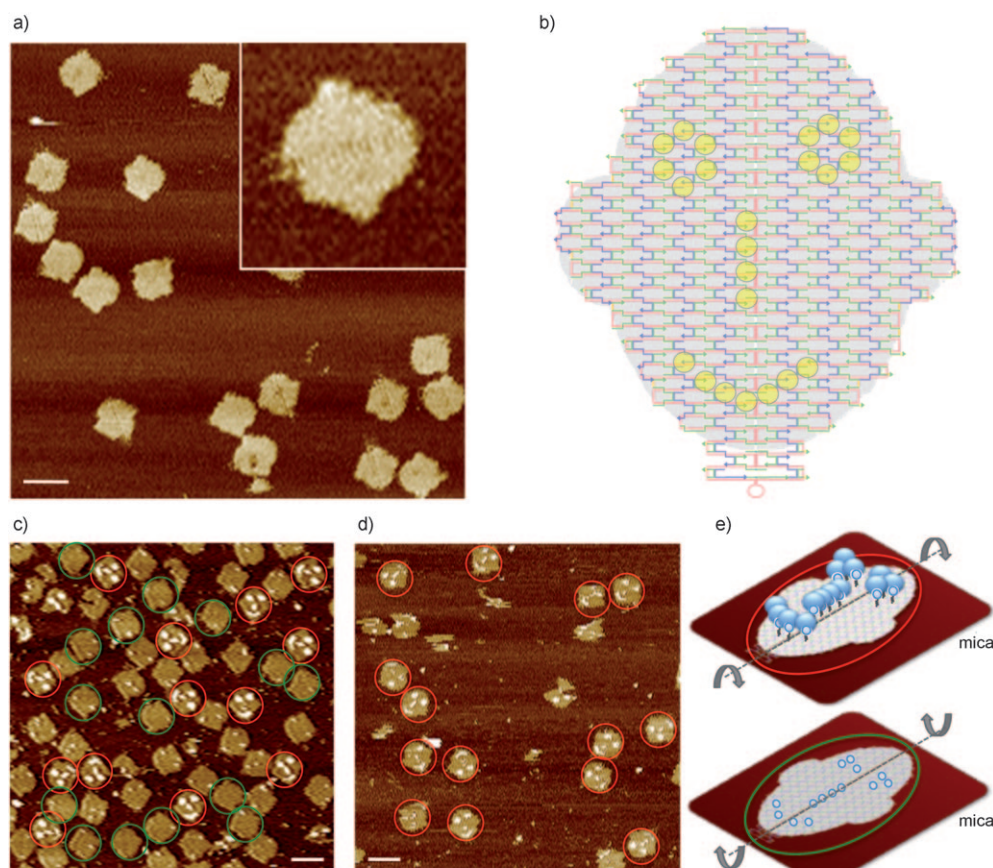


Figure 2. a) AFM characterization of the unmodified DNA origami. The inset shows a magnified structure, which reveals a less-defined and floppy region at the bottom of the head which corresponds to the 44-nucleotide-long hairpin loop of the M13mp18 scaffold, as well as the central seam of the structure. b) Schematic representation of the DNA-origami design. The circular M13mp18 scaffold and staple strands are represented by red and green/blue strands, respectively. Yellow circles represent positions in which biotin, BG, or CH tags were incorporated. Structures containing 23 biotinylated staples were coupled with STV either c) subsequent to the adsorption of origami onto mica or d) in homogeneous solution, followed by adsorption of the origami onto mica. While the former procedure leads to equally distributed face-up- or face-down-oriented arrangements presenting the biotin groups to the solution phase or surface, respectively (upper and lower panel in (e), respectively), the latter method produces almost exclusively face-up-oriented structures (scale bars = 100 nm).

origami was also confirmed by gel electrophoretic analysis (see Figure S5 in the Supporting Information). Statistical analysis of various AFM images indicated that average coupling efficiencies were about 60 % for both mSTV and Snap-tag fusion proteins and 35 % for HaloTag fusions (see Table S9 in the Supporting Information).^[29]

To illustrate how the scope of our approach can be broadened further we demonstrate that orthogonal tags can also be installed on both sides of the quasi two-dimensional plane of DNA origami. We designed a Janus face by taking advantage of the helical-twist color code provided by the SARSE software (see Figure S6 in the Supporting Information), in which our initial design (Figure 2b) was modified to present additional biotin groups arranged in stripes on the reverse side of the smiley face. While theoretical design predicted the formation of two clearly distinguishable protein patterns on the two sides of the origami (see Figure S7 in the Supporting Information), AFM analysis revealed that many

structures indeed showed both patterns on one side (see Figure S8 in the Supporting Information). Closer inspection of the helical-twist color code of the SARSE representation and comparison with three-dimensional models suggested that the SARSE color coding does not always correspond to real orientations of individual nucleotides within the folded origami. An adjustment of the design (see Figure S9 in the Supporting Information) then enabled assembly of the desired Janus origami, with the expected two different faces observed in the AFM analysis (Figure 4a–c).

To demonstrate orthogonal protein decoration of the two Janus faces we assembled two different origami structures that presented STV molecules on either their front or the reverse side (denoted as **m-CH,BG,4b_f** or **j-CH,BG,9b_b**, respectively; see Figures S4 and S10 in the Supporting Information, respectively), in addition to mKate-Snap and EYFP-Halo proteins installed on the front side of the structures (Figure 4d). We expected that STV-mediated

binding to biotinylated surfaces should orient the two superstructures such that mKate-Snap and EYFP-Halo proteins are pointing either towards the surface (**m-CH,BG,4b_f**) or the solution phase (**j-CH,BG,9b_b**). Consequently, the accessibility of mKate-Snap and EYFP-Halo for immunological detection should differ significantly for the two different origamis. This assumption was tested by immobilizing approximately equal amounts of **m-CH,BG,4b_f** and **j-CH,BG,9b_b** in microplates coated with biotinylated bovine serum albumin. Immobilized origami was quantified by the polymerase chain reaction (qPCR), using primers specific for the M13mp18 DNA backbone of the origami (blue bars in Figure 4d). Comparison with a control origami lacking any STV molecules clearly indicated that both **m-CH,BG,4b_f** and **j-CH,BG,9b_b** were capable of specific binding to the biotinylated surface (see Figure S11 in the Supporting Information). The accessibility of mKate-Snap and EYFP-Halo proteins was tested by probing the immobi-

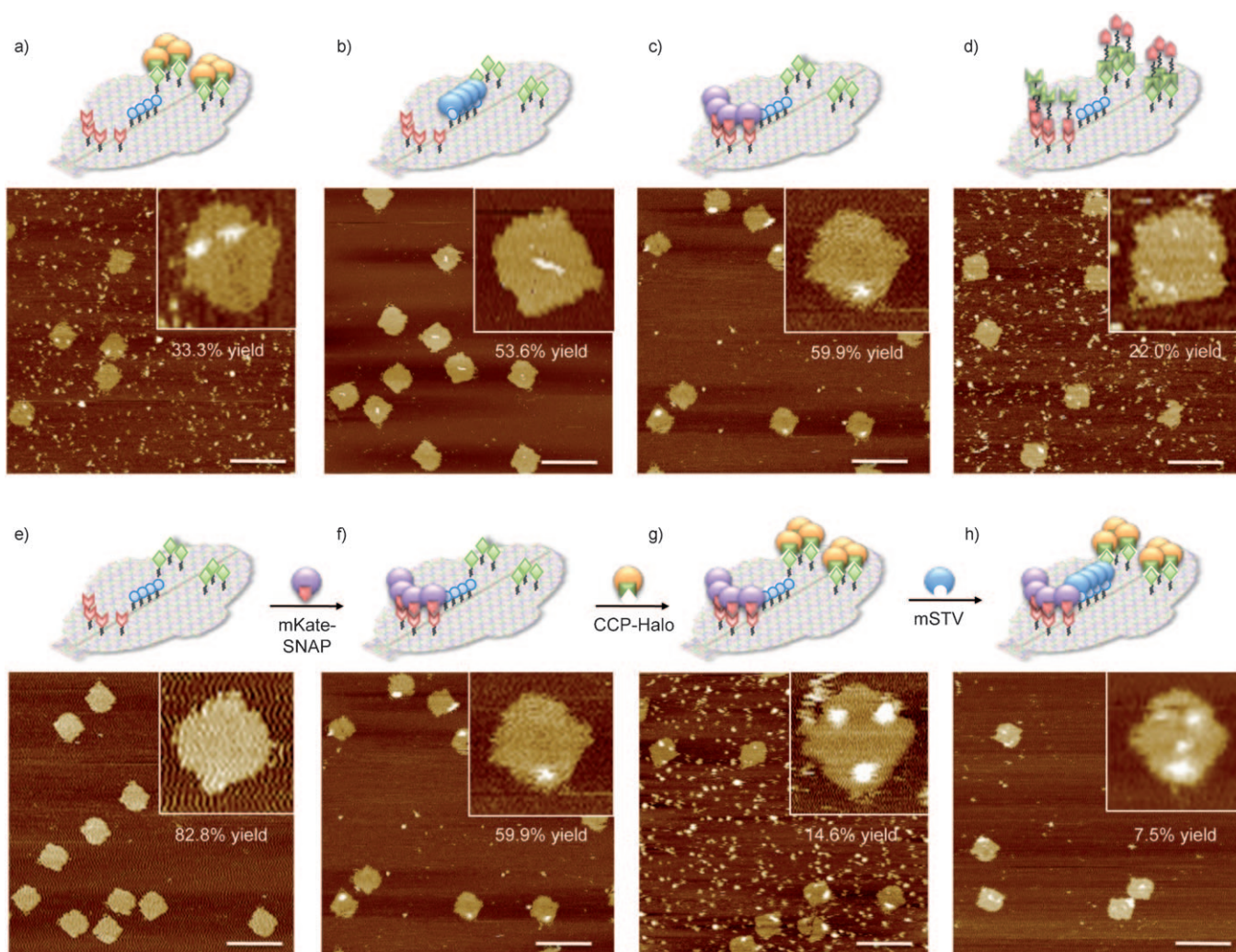


Figure 3. Schematic representations and AFM images of orthogonal modified DNA origami. Examples of monofunctionalized DNA–origami conjugates are shown for a) CCP-Halo, b) mSTV, and c) mKate-Snap. d) The binding of covalin leads to modification of both the eye and mouth features. Consecutive orthogonal protein binding is demonstrated by incubation of e) CH-, biotin-, and BG-bearing origami with f) mKate-Snap (indicated by violet spheres), g) CCP-Halo (yellow spheres), and h) mSTV (blue spheres). The binding of these proteins led to decoration of the origami with features resembling a mouth, eyes, and a nose, respectively. Magnifications of representative origami structures are shown as insets. The yields obtained in the sequential formation of the target structures are given with respect to the total of well-formed structures (see also Table S9 in the Supporting Information). Scale bars are 100 nm.

lized origami with specific IgG antibodies from rabbit (denoted as α -Snap AB or α -EYFP AB, respectively; Figure 4d) and a secondary reagent for immuno-PCR (IPCR) detection of rabbit IgG^[30] (CHI-rabbit conjugate, Chimera Biotech). Comparison of the IPCR and qPCR signals (blue and red bars, respectively, in Figure 4d) clearly shows that the IPCR signals are significantly greater in the case of the Janus origami (**j-CH,BG,9b_i**) than those obtained from the origami presenting all proteins on one side (**m-CH,BG,4b_i**), although this origami was immobilized in equal (α -Snap AB detection) or even larger amounts (α -EYFP AB) than the Janus origami. To the best of our knowledge, this is the first demonstration that DNA origami can be specifically decorated with proteins on both sides of its quasi-two-dimensional plane and that this approach is useful for the directional immobilization of DNA nanostructures.

In conclusion, we demonstrate here that self-labeling fusion proteins can be used for the site-selective decoration of DNA nanostructures. As a consequence of its orthogonal specificity, this protein labeling technique holds the potential for the use of unpurified proteins from crude cell lysates.^[20,21] We therefore anticipate that the approach will allow DNA superstructures to be readily decorated with complex patterns of arbitrary proteins. This orthogonal protein coupling will open up ways to control the accessibility and reactivity of distinctive protein arrangements presented on selected surface areas of DNA scaffolds.

Received: September 21, 2010
Published online: October 28, 2010

Keywords: DNA structures · nanostructures · proteins · self-assembly

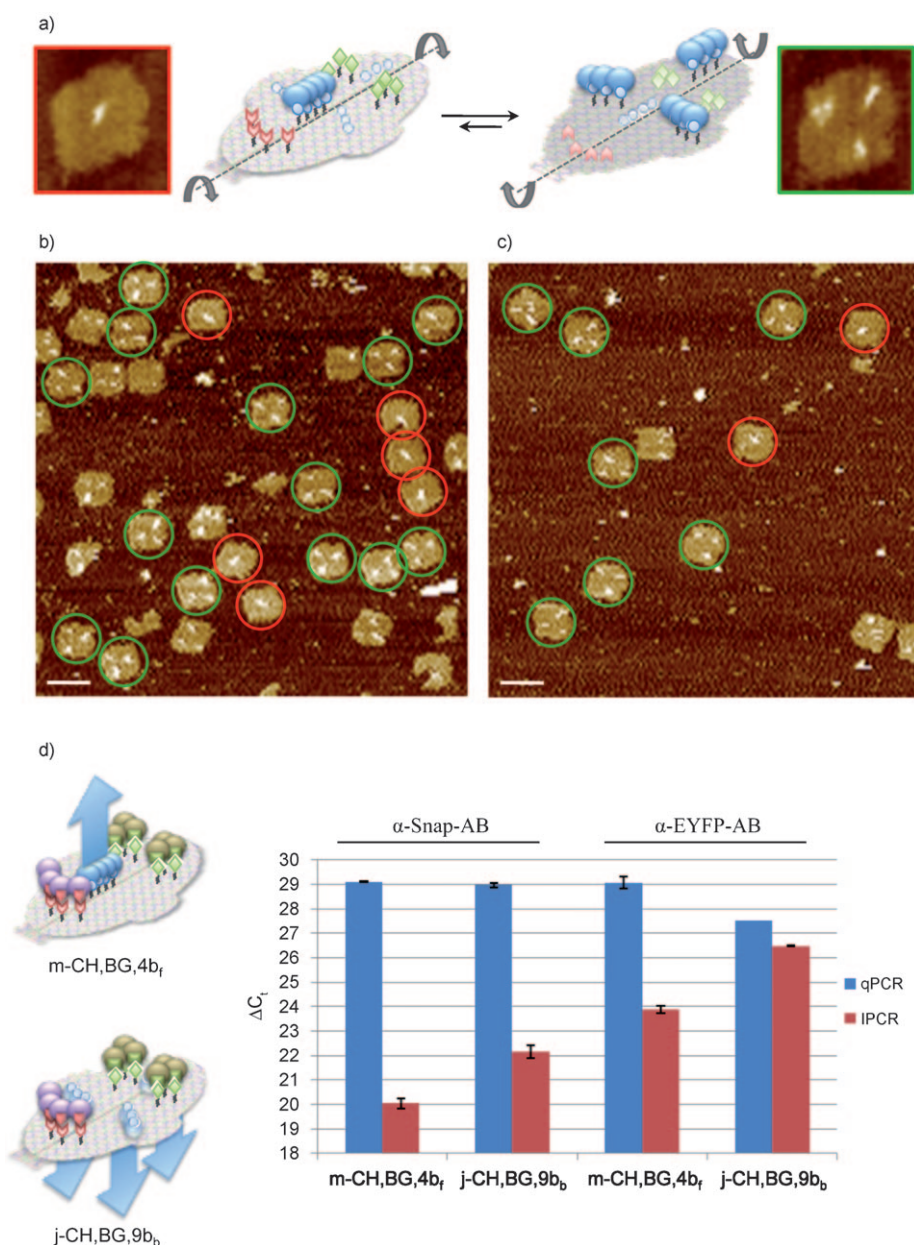


Figure 4. Illustration of Janus origami, which presents distinguishable topological patterns on the two sides. a) The front side face bears BG-tags and CH-tags, similar to as shown in Figure 2b, with four biotin groups as the nose feature, while the reverse face presents nine biotin groups arranged in three stripes. Binding of STV to Janus origami, either b) subsequent c) or prior to adsorption on mica, leads to formation of the two expected protein patterns. In the AFM images, the front and back faces are indicated by red and green circles, respectively; scale bars are 100 nm. d) Orthogonal protein decoration of the two faces of Janus origami is demonstrated by directional surface binding of two different origami structures that present STV molecules on either their front or back side (**m-CH,BG,4b** or **j-CH,BG,9b**, respectively), as well as mKate-Snap and EYFP-Halo proteins installed at the front side. The blue arrows in the schematic representations of the origamis on the left represent the proposed directionality of STV-mediated binding to biotinylated surfaces. Immobilized **m-CH,BG,4b** or **j-CH,BG,9b** origami was quantified by qPCR (blue bars), and mKate-Snap or EYFP-Halo proteins were detected by using specific antibodies (α -Snap AB or α -EYFP AB, respectively) and IPCR signal amplification (red bars). ΔC_t values are proportional to the amount of detectable origami or proteins (blue or red bars, respectively). Note that the IPCR signals are significantly greater in the case of Janus origami (**j-CH,BG,9b**) than those obtained from **m-CH,BG,4b**. For additional controls see Figure S12 in the Supporting Information.

- [1] N. C. Seeman, *Mol. Biotechnol.* **2007**, 37, 246–257.
- [2] C. Lin, Y. Liu, H. Yan, *Biochemistry* **2009**, 48, 1663–1674.
- [3] P. W. Rothmund, *Nature* **2006**, 440, 297–302.
- [4] E. S. Andersen, M. Dong, M. M. Nielsen, K. Jahn, R. Subramani, W. Mamdouh, M. M. Golas, B. Sander, H. Stark, C. L. Oliveira, J. S. Pedersen, V. Birkedal, F. Besenbacher, K. V. Gothelf, J. Kjems, *Nature* **2009**, 459, 73–76.
- [5] H. Dietz, S. M. Douglas, W. M. Shih, *Science* **2009**, 325, 725–730.
- [6] S. M. Douglas, H. Dietz, T. Liedl, B. Hogberg, F. Graf, W. M. Shih, *Nature* **2009**, 459, 414–418.
- [7] C. M. Niemeyer, *Angew. Chem.* **2010**, 122, 1220–1238; *Angew. Chem. Int. Ed.* **2010**, 49, 1200–1216.
- [8] Y. He, Y. Tian, A. E. Ribbe, C. Mao, *J. Am. Chem. Soc.* **2006**, 128, 12664–12665.
- [9] B. A. R. Williams, K. Lund, Y. Liu, H. Yan, J. C. Chaput, *Angew. Chem.* **2007**, 119, 3111–3114; *Angew. Chem. Int. Ed.* **2007**, 46, 3051–3054.
- [10] R. Chhabra, J. Sharma, Y. Ke, Y. Liu, S. Rinker, S. Lindsay, H. Yan, *J. Am. Chem. Soc.* **2007**, 129, 10304–10305.
- [11] S. Rinker, Y. Ke, Y. Liu, R. Chhabra, H. Yan, *Nat. Nanotechnol.* **2008**, 3, 418–422.
- [12] C. M. Niemeyer, W. B rger, J. Peplies, *Angew. Chem.* **1998**, 110, 2391–2395; *Angew. Chem. Int. Ed.* **1998**, 37, 2265–2268.
- [13] O. I. Wilner, Y. Weizmann, R. Gill, O. Lioubashevski, R. Freeman, I. Willner, *Nat. Nanotechnol.* **2009**, 4, 249–254.
- [14] H. Yan, S. H. Park, G. Finkelstein, J. H. Reif, T. H. LaBean, *Science* **2003**, 301, 1882–1884.
- [15] H. Li, S. H. Park, J. H. Reif, T. H. LaBean, H. Yan, *J. Am. Chem. Soc.* **2004**, 126, 418–419.
- [16] K. Lund, Y. Liu, S. Lindsay, H. Yan, *J. Am. Chem. Soc.* **2005**, 127, 17606–17607.
- [17] A. Kuzuya, M. Kimura, K. Numa-jiri, N. Koshi, T. Ohnishi, F. Okada, M. Komiyama, *ChemBioChem* **2009**, 10, 1811–1815.
- [18] N. V. Voigt, T. Topping, A. Rotaru, M. F. Jacobsen, J. B. Ravnsbaek, R. Subramani, W. Mamdouh, J. Kjems, A. Mokhir, F. Besenbacher, K. V. Gothelf, *Nat. Nanotechnol.* **2010**, 5, 200–203.

- [19] K. Numajiri, T. Yamazaki, M. Kimura, A. Kuzuya, M. Komiyama, *J. Am. Chem. Soc.* **2010**, *132*, 9937–9939.
- [20] A. Keppler, S. Gendreizig, T. Gronemeyer, H. Pick, H. Vogel, K. Johnsson, *Nat. Biotechnol.* **2003**, *21*, 86–89.
- [21] G. V. Los, K. Wood, *Methods Mol. Biol.* **2007**, *356*, 195–208.
- [22] F. Kukulka, C. M. Niemeyer, *Org. Biomol. Chem.* **2004**, *2*, 2203–2206.
- [23] N. C. Shaner, R. E. Campbell, P. A. Steinbach, B. N. Giepmans, A. E. Palmer, R. Y. Tsien, *Nat. Biotechnol.* **2004**, *22*, 1567–1572.
- [24] L. Fruk, V. Rajendran, M. Spengler, C. M. Niemeyer, *Chem-BioChem* **2007**, *8*, 2195–2198.
- [25] Y. Huang, M. Humenik, M. Sprinzl, *Protein Expression Purif.* **2007**, *54*, 94–100.
- [26] C. Chidley, K. Mosiewicz, K. Johnsson, *Bioconjugate Chem.* **2008**, *19*, 1753–1756.
- [27] M. Howarth, D. J. Chinnappen, K. Gerrow, P. C. Dorrestein, M. R. Grandy, N. L. Kelleher, A. El-Husseini, A. Y. Ting, *Nat. Methods* **2006**, *3*, 267–273.
- [28] E. S. Andersen, M. Dong, M. M. Nielsen, K. Jahn, A. Lind-Thomsen, W. Mamdouh, K. V. Gothelf, F. Besenbacher, J. Kjems, *ACS Nano* **2008**, *2*, 1213–1218.
- [29] Systematic optimization of coupling efficiencies by varying the protein concentration and coupling stoichiometry led to the protocol given in the Supporting Information. Preliminary experiments indicate that inclusion of, for example, oligoethylene glycol spacers between the reactive BG or CH group and the DNA scaffold improve the coupling yields. However, it was observed in this study that the charge of the proteins significantly influences the coupling efficiency. In particular, proteins with a lower isoelectric point (pI) bind less efficiently than those with higher pI values, thereby suggesting that electrostatic repulsion between the negatively charged origami and proteins plays an important role for protein binding.
- [30] C. M. Niemeyer, M. Adler, R. Wacker, *Nat. Protoc.* **2007**, *2*, 1918–1930.